Laboratory Study on Gasification Reactivity of Coals and Petcokes in CO2/Steam at High Temperatures

ARTICLE *in* ENERGY & FUELS · SEPTEMBER 2013

Impact Factor: 2.79 · DOI: 10.1021/ef400373y

4 AUTHORS, INCLUDING:

Liwei Ren
Handan College
1 PUBLICATION **8** CITATIONS
SEE PROFILE

Jianli Yang
Chinese Academy of Sciences
56 PUBLICATIONS **631** CITATIONS
SEE PROFILE

energy&fuels

Article

pubs.acs.org/EF

Laboratory Study on Gasification Reactivity of Coals and Petcokes in CO_2/Steam at High Temperatures

Liwei Ren,[†,‡] Jianli Yang,[†,*] Feng Gao,[§] and Jinding Yan[∥]

[†]State Key Laboratory of Coal Conversion, Institute of Coal Chemistry, Chinese Academy of Sciences, Taiyuan 030001, P.R. China

[‡]University of Chinese Academy of Sciences, Beijing 100049, P.R. China

[§]College of Material Science and Engineering, Taiyuan University of Technology, Taiyuan 030024, P.R. China

[∥]Basic Research Service, Ministry of Science and Technology of the People's Republic of China, Beijing 100862, P.R. China

ABSTRACT: The gasification reactivity of 13 carbonaceous materials in CO_2 or in steam was studied in the temperature range 1000−1600 °C. The gasification reaction was carried out in a drop-in-fixed-bed reactor under atmospheric pressure. The gasifying agent fed into the reactor either as pure gas or as 36% volumetric concentration in argon with a total gas flow rate of 500 mL/min. The test samples included different rank coals, petcokes, and graphites. The raw materials were used to eliminate the problem related to char prepreparation. The dynamic profiles of gasification rate were used to compare the gasification behaviors for different samples. The physicochemical characteristics of chars were evaluated by scanning electron microscopy and N_2 adsorption method. The experimental results reveal that the difference in gasification reactivity among samples decreases as the temperature increases and is not distinguishable for most coals at 1600 °C. However, the temperature is still critical for gasification of petcokes and some high-rank coals at high temperature. The gasification reactivity of petcokes is 2−9 times lower than that of coals at 1600°C. The kinetic analysis reveals that the temperature dependence of reactivity varies with the type of materials. It is interested to find that, in the temperature range 1400−1600 °C, the gasification reactivity in CO_2 is higher than that in steam for coals but not for petcokes. From the views of the reaction thermodynamics, the gas diffusion difficulty, and the catalytic effect, the high temperature is favorable to the CO_2-gasification. The effect of AAEMs (alkali and alkaline earth metals) should be a key factor. The content of AAEMs is apparent in coals but limited in petcokes. The Arrhenius plots reveal that the gasification mechanism may be altered around 1200 °C for most of coals. The petcokes are appeared with the most compact physical structure and the least gasification reactivity. Either the shrinking core model (SCM) or the volume reaction model (VRM) is suitable for most of the samples and conditions but not suitable for the petcokes. A diffusion term associated with the carbon structure may be needed for modelling the gasification behaviors of the petcoke-like materials.

1. INTRODUCTION

Gasification technology is used to convert feedstocks, not only coal but also petcoke and other carbonaceous materials, to fuel gas or syngas,[1,2] which can be used to generate electricity and heat or to synthesize liquid fuel and chemicals.[3] With the increased demand of gasification capacity and the increased requirement of using a wide range of feedstocks, the development of gasification technology is heading toward the direction of large-scale systems and feedstock flexibility.

The entrained-flow gasification, as a modern gasification technology, has been widely used around the world nowadays due to its high performance (in terms of high carbon conversion, high capacity, and feedstock flexibility).[4] The entrained-flow gasifier is operated at high-temperature (1200−1700 °C) and high-pressure (2−6.5 MPa) conditions. The feed points for feedstock and gasifying agents (O_2 or air and steam) are closely spaced. Pulverized particles (dry or coal−water slurry) fed into the gasifier reach slagging temperatures in a few seconds. The evaporation of water, the pyrolysis of volatiles, the combustion and gasification of volatiles and in situ produced char (also referred to as carbon), as well as the reactions involving heteroatoms take place immediately. Because of the high temperatures employed, the low-gasification-reactivity feedstocks may be applied.

As an indispensable parameter, many researchers have pointed out the importance of the gasification reactivity of feedstocks to gasifier performance and efficiency.[5−7] The gasification reactivity of feedstocks can be affected by many factors.[7] The type of feedstocks and the operation condition are the main factors. The mineral matter in feedstocks may catalyze the gasification reaction, and the catalytic effect of mineral matter plays an important role on gasification rate, especially at lower temperatures.[8,9]

Despite the complexity of reactions involved in the gasification process, the gasification reactivity of feedstocks is dependent on the char-gasification reactions (R-1 and R-2). The former is the CO_2-gasification reaction (known as the Boudouard reaction), and the latter is the steam-gasification reaction. Both reactions determine the gasifier residence time due to the devolatilization, and combustion reactions are much faster and the direct hydrogenation reaction is limited at high temperature.[10] In addition, the water gas shift reaction R-3 may be accompanied.

$$C + CO_2 \rightarrow 2CO \quad \text{(R-1)}$$

$$C + H_2O \rightarrow CO + H_2 \quad \text{(R-2)}$$

Received: March 4, 2013
Revised: July 20, 2013
Published: July 30, 2013

Table 1. Proximate and Ultimate Analyses of the Test Samples[a]

	proximate (wt %)			ultimate (wt %, daf)				
samples	A_d	V_d	FC_d	C	H	O*	N	S_t
XLT(LRC1)	10.34	42.86	46.80	77.20	4.81	15.51	1.26	1.22
SL(LRC2)	43.16	27.98	28.86	75.40	4.75	17.43	1.22	1.20
WS(LRC3)	18.76	36.26	44.98	78.27	4.81	14.00	1.62	1.31
TL(LRC4)	42.12	23.34	34.54	79.90	5.55	12.87	1.04	0.63
YM(LRC5)	20.32	33.3	46.38	80.18	4.32	12.29	0.86	2.35
XCG(MRC1)	4.11	34.84	61.05	81.73	4.73	12.06	1.23	0.25
GP(HRC1)	22.84	9.14	68.02	88.06	3.81	6.30	1.36	0.47
YQ(HRC2)	20.58	6.91	72.51	89.48	3.01	4.07	1.21	2.24
QS(HRC3)	8.53	5.85	85.62	91.32	2.92	4.51	0.95	0.30
YS(PC1)	0.88	7.99	91.13	88.97	3.12	5.54	1.01	1.36
JS(PC2)	1.54	9.83	88.63	84.98	1.90	5.79	0.93	6.40
graphite(GR1)	0.16	2.11	97.73	99.12	–	0.49	–	0.39
graphite(GR2)	3.82	1.76	94.42	99.31	–	0.28	0.06	0.35

[a]A: ash; V: volatile matter; FC: fixed carbon; d: dry basis; daf: dry ash-free basis; *: by difference; –: not detected; LRC: low-rank coal; MRC: mid-rank coal; HRC: high-rank coal; PC: petcoke; GR: graphite.

$$CO + H_2O \leftrightarrow CO_2 + H_2 \quad \text{(R-3)}$$

For an industry gasifier, the heat is supplied by combustion or partial combustion of feedstock. In a laboratory bench-scale study, the heat for a gasification reactor is usually not supplied by combustion but by an external source of heat. Therefore, the preprepared char is often used to minimize the complexity and for decoupling the processes. However, the gasification reactivity of the preprepared char has a strong dependence on preparation conditions.[11−13] The type of volatiles released and the release process during char formation govern the carbon structure and morphology of the char, which in turn affect the gasification reactivity of the char.[7,14,15] There is an apparent lack of fundamental understanding of the gasification behavior of the in situ chars, especially when temperature is higher than 1400 °C. Detailed understanding of the gasification reactivity at high temperature for chars derived from the different sources under different conditions is necessary.

The gasification temperature is the most important parameter affecting the gasification reactivity of chars. Many studies can be found in the literature. The gasification kinetics changes with the gasification temperature. It is believed that the gasification process is controlled by the carbon-gasification reaction when the temperature is lower than 1000 °C,[2,7] while the process is controlled by pore diffusion when the temperature is higher than 1150 °C.[16−18] It was, however, also reported that the gasification reactivity of chars has a strong tendency of increasing with the increase of temperature from 1000 to 1400 °C.[19]

It is commonly observed that at the lower temperatures the difference of gasification reactivity among different feedstocks is apparent and the apparent activation energies are relatively high, while at the higher temperatures the difference of gasification reactivity among different feedstocks is less significant and the apparent activation energies are relatively low. It is, therefore, believed that at the lower temperatures the controlling step is the carbon-gasification reaction, while at the higher temperatures the controlling step is the gas diffusion. In the entrained-flow gasifier, however, although the gasification reactivity for most coals is not a problem due to its high operation temperatures, the carbon conversion rate for some feedstocks (such as some high-rank coals and petcokes) is not satisfied. It is certain that petcoke, derived from oil refinery coke units or other cracking processes, has a much lower gasification reactivity than coal chars, especially at low temperatures.[20,21] Finding an effective way to use the petcoke as a suitable feedstock for fuel gas or syngas production is desired. Furthermore, the notable difference in gasification reactivity for chars from different coals and different preparation conditions is found not only at low temperatures (750−1000 °C)[7,22] but also at high temperatures (1150−1400 °C).[18,19,23] The carbon structure of chars must play an important role.

The main objective of this work is to investigate the gasification reactivity of a wide range of solid carbonaceous materials with respect to CO_2 or steam in the temperature range 1000−1600 °C under atmospheric pressure. The experiments were carried out in a drop-in-fixed-bed reactor, which can heat the samples to the desired temperature in about 2 s with an electric heater. The raw samples were directly fed into the reactor to avoid the problems from prepreparation of chars. Mass spectrometry (MS) was used to monitor gaseous products continually. A dynamic evolution profile of gasification rate was used to represent the gasification reactivity quantitatively. The physicochemical properties of raw samples and their residual chars were related with the corresponding gasification reactivity. In addition, the gasification kinetics of various samples was also analyzed.

2. EXPERIMENTAL SECTION

2.1. Test Samples. Eleven solid carbonaceous materials, including low-rank coal (XLT, SL, WS, TL, and YM), mid-rank coal (XCG), high-rank coal (GP, YQ, and QS), and petcoke (YS and JS) were tested. In addition, two types of graphite (GR1 and GR2) were also tested for comparison. The samples were crushed and dried under vacuum at 110 °C for 24 h. Particles with 50 ± 1 mg in weight (about 2−4 mm in diameter, depending on the density of sample) were selected as the test samples. Proximate and ultimate analyses of the test samples are listed in Table 1.

2.2. Experimental Setup and Procedures for Gasification Reaction. The gasification experiments were carried out in a drop-in-fixed-bed reactor equipped with a controllable electric heater (Figure 1). A corundum tube (18 mm in inside diameter and 1250 mm in length) was used as the reaction tube. The constant-high-temperature zone is about 100 mm and located at the middle of the reactor. The reaction tube was placed in the reactor vertically. Corundum beads with an average diameter of 1 mm were piled up in the reaction tube from the bottom. A sample holder with a letdown valve was located on the top of

dx.doi.org/10.1021/ef400373y | Energy Fuels 2013, 27, 5054−5068

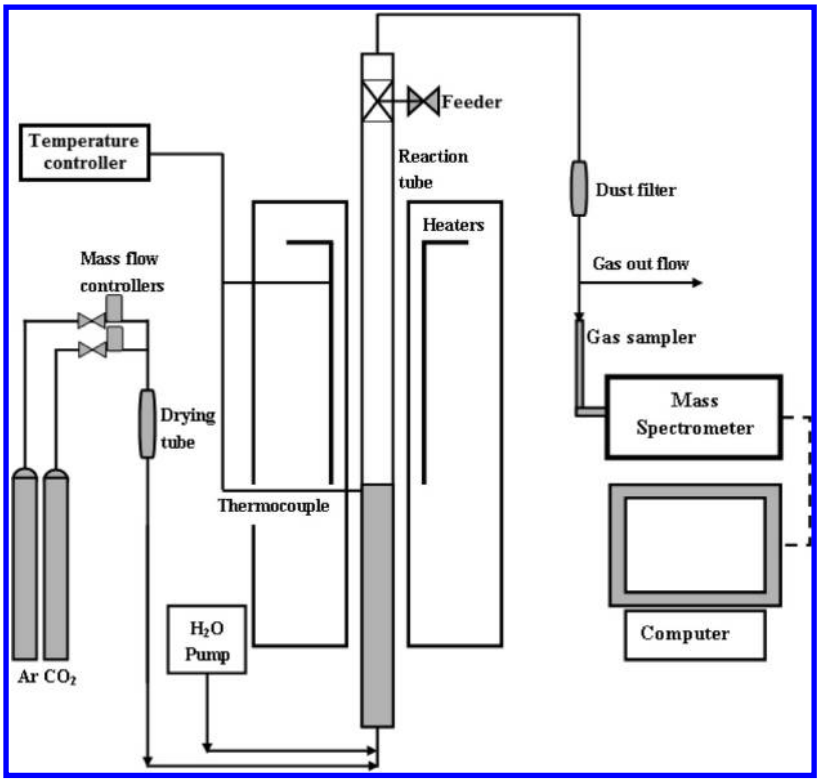

Figure 1. Schematic diagram of the drop-in-fixed-bed reactor system.

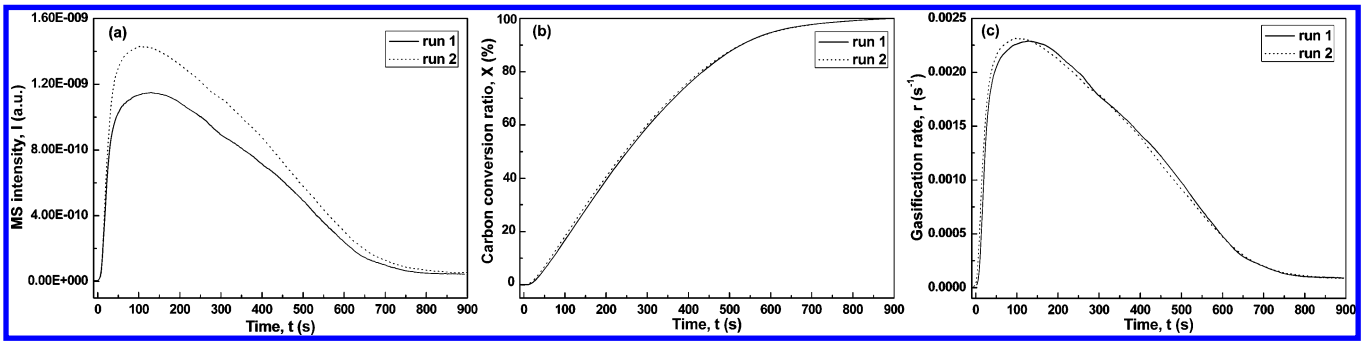

Figure 2. Illustration of the data process procedure (CO_2-gasification of graphite): (a) the CO profiles collected by MS (I–t), (b) the normalized integral-profiles (X–t), and (c) the differential-profiles (r–t).

the reaction tube. The gas was feed into the reaction tube from the bottom, and the sample was charged from the top.

A single particle was preplaced on the sample holder. When the reactor stabilized at the desired temperature, the letdown valve of the sample holder was switched to open and allowed the sample particle dropping into the reaction tube and sitting on the corundum-beads-bed in about 0.45–0.51 s (estimated by considering the effect from both sample gravity and gas drag force), on which the particle reached a desired temperature (1000–1600 °C) in about 2 s (estimated according to the heat balance calculation).

The gasification reaction was carried out under atmospheric pressure. During the experiment, gasifying agent, CO_2 (100% or 36% in Ar) or steam (36% in Ar) was continuously supplied into the reaction tube with a total flow rate of 500 mL/min, which was selected to avoid the influence of the gas flow rate on the gasification reaction. The gaseous products were swept into an online gas analyzer (MS, OmniStar GSD320 mass spectrometer of PFEIFFER-VACUUM) by the gas flow and monitored continuously. The sample particle was left in the reactor until the gasification reaction was completed. After the reactor was cooled down to room temperature, the residuals were discharged from the reactor through the valve at the bottom of the reaction tube.

2.3. Data Processing and Reproducibility. The carbon conversion ratio was calculated based on the CO profile (if CO_2 as the gasifying agent) or CO and CO_2 profiles (if steam as the gasifying agent) recorded by the online MS. It can be assumed that the peak area of the CO profile or the CO_2 profiles from MS is proportional to the amount of CO or CO_2 produced during the reaction. The carbon conversion ratio can be calculated by eq 1 or eq 2 as follows:

For the CO_2-gasification:

$$X = \frac{n_{t,\mathrm{CO}}}{n_{\mathrm{total,CO}}} = \frac{k_{\mathrm{CO}} S_{t,\mathrm{CO}}}{k_{\mathrm{CO}} S_{\mathrm{total,CO}}} = \frac{S_{t,\mathrm{CO}}}{S_{\mathrm{total,CO}}} \quad (1)$$

For the steam-gasification:

$$X = \frac{n_{t,\mathrm{CO}} + n_{t,\mathrm{CO_2}}}{n_{\mathrm{total,CO}} + n_{\mathrm{total,CO_2}}} = \frac{S_{t,\mathrm{CO}} + \frac{k_{\mathrm{CO_2}}}{k_{\mathrm{CO}}} S_{t,\mathrm{CO_2}}}{S_{\mathrm{total,CO}} + \frac{k_{\mathrm{CO_2}}}{k_{\mathrm{CO}}} S_{\mathrm{total,CO_2}}} \quad (2)$$

where X is carbon conversion ratio; $n_{\mathrm{total,CO}}$ and $n_{\mathrm{total,CO_2}}$ are the total amount of CO and CO_2 produced, respectively; $n_{t,\mathrm{CO}}$ and $n_{t,\mathrm{CO_2}}$ are the amount of CO and CO_2 produced from time 0 to time t, respectively;

dx.doi.org/10.1021/ef400373y | Energy Fuels 2013, 27, 5054–5068

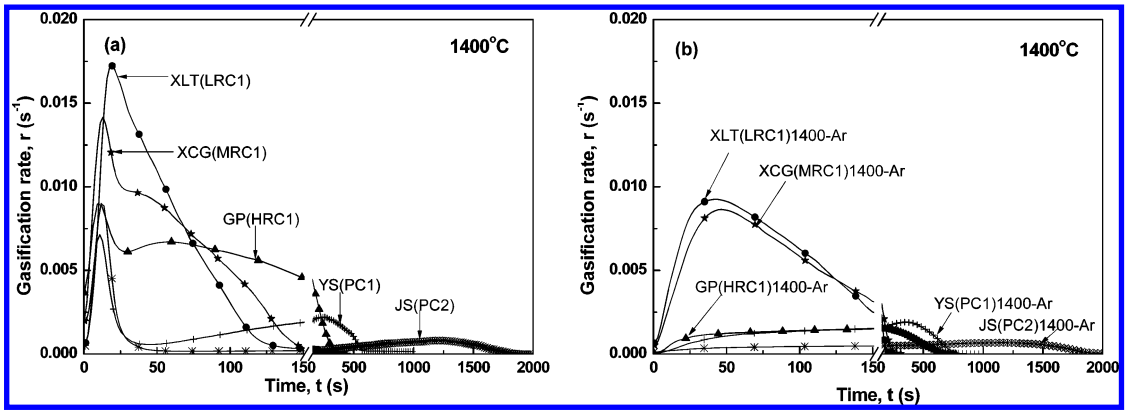

Figure 3. Comparison of the CO_2-gasification rate profiles of (a) raw samples and (b) preprepared chars at 1400 °C under atmospheric pressure.

$S_{total,CO}$ and S_{total,CO_2} are the total peak areas of CO and CO_2, respectively; $S_{t,CO}$ and S_{t,CO_2} are the peak areas of the CO and CO_2 profiles from time 0 to time t, respectively; and k_{CO} and k_{CO2} are the corresponding coefficients for the peak areas of CO and CO_2, respectively. The gasification rate, r, is defined as the differential of the carbon conversion ratio with respect to time and can be derived from eq 1 or eq 2 as follows:

$$r = \frac{dX}{dt} = \frac{1}{S_{total,CO}} \frac{dS_{t,CO}}{dt} \quad (3)$$

$$r = \frac{dX}{dt} = \frac{1}{S_{total,CO} + \frac{k_{CO_2}}{k_{CO}} S_{total,CO_2}} \frac{d\left(S_{t,CO} + \frac{k_{CO_2}}{k_{CO}} S_{t,CO_2}\right)}{dt} \quad (4)$$

The data process procedure is illustrated in Figure 2, which can also be used to confirm the repeatability of the method. The gasification of graphite in CO_2 is used as an example, in which the main chemical reaction involved is R-1. Figure 2a is the CO profile collected by MS after the graphite particle drop into the reaction tube. The profiles in Figure 2b are the normalized integral-profiles obtained according to eq 1, which depict the change of carbon conversion ratio with respect to time. The profiles in Figure 2c are the differential-profiles obtained according to eq 3, which represent the change of gasification rate with respect to time. The difference between the two runs in Figure 2a is due to the difference in sample weight (47.3 mg for run 1 and 56.8 mg for run 2). Comparing the carbon conversion ratio profiles (shown in Figure 2b) or the gasification rate profiles (shown in Figure 2c) from two runs, it can be seen that the repeatability of the experiments is acceptable. Nevertheless, the data profiles used in this study are the most representative one of three runs.

2.4. Sample Characterization. The surface morphology of samples was examined by scanning electron microscopy (SEM, JSM-35C) under an acceleration voltage of 25 kV. The pore structure of the distribution of samples was analyzed based on N_2 sorption data, which is measured by an autoadsorption analyzer (3H-2000PS) at 77 K.

3. RESULTS AND DISCUSSION

3.1. Difference in Gasification Reactivity of In Situ Char and Preprepared Char. It is common understanding that the gasification behavior of the preprepared char may be significantly different from that of in situ formed char, although many related experiments start with the preprepared char. The gasification reactivity of chars depends on their formation conditions, such as temperature, heating rate, as well as residence time.[24,25] Some studies, therefore, use the raw material as the starting sample instead of the preprepared char.[13]

The CO_2-gasification reactivity of the raw samples and their preprepared chars (prepared at 1400 °C under Ar atmosphere for 5 min in the drop-in-fixed-bed reactor) is compared in Figure 3. The gasification reactivity is presented as a gasification rate profile, which develops with the reaction time and depicts the characteristics of organic volatile and in situ char at different reaction stages. The test samples include XLT(LRC1), XCG(MRC1), GP(HRC1), YS(PC1), and JS(PC2). The corresponding preprepared chars are marked as XLT(LRC1)1400-Ar, XCG(MRC1)1400-Ar, GP(HRC1)1400-Ar, YS(PC1)1400-Ar, and JS(PC2)1400-Ar, respectively.

It can be seen that the dynamic profile can provide the reaction progress at any stage over the whole reaction course. It is clear that the profiles for raw samples and their preprepared chars are distinctly different. Except for sample XLT(LRC1), the gasification rate profiles for samples XCG (MRC1), GP(HRC1), YS(PC1) and JS(PC2) have two distinct peaks: a sharp peak at the early stage of the reaction followed by a broad peak with the lower intensity. The first peak is overlapped with the second peak for coal samples. The two peaks are well resolved for petcoke samples. However, no sharp peak can be found for the preprepared chars, and the gasification reactivity of the preprepared chars is generally lower than that of the raw sample feeds.

The two distinct peaks in the gasification rate profiles for the raw sample feeds are corresponding to two carbon-containing group compositions: volatiles and char. Both the coal and petcoke contain a certain amount of volatiles or volatilizable substances, which are removed during the preparation process for preprepared char. According to the thermodynamic analysis, the organic volatiles such as light alkanes and light aromatic hydrocarbons react with CO_2 more readily than char under the experimental conditions. The first peak is, therefore, related to two reactions: the volatiles reforming and the in situ char-gasification. The following broad peak is only attributed to the in situ char-gasification. Only one peak can be found in the rate profile for sample XLT(LRC1). The transition from the region involving reactions of both volatiles and char to the region of char reaction is gradual for this sample.

In comparison with the preprepared char, the gasification reactivity of the in situ char is generally higher. In order to eliminate the difference caused by char preparation, the raw sample particle was used in this study.

3.2. Feeding Size Selection. In order to eliminate the sample particle sticking on the side of the reaction tube, a single particle as the feed was selected. However, the size of the particle needs to be carefully selected to avoid the size influence. The

dx.doi.org/10.1021/ef400373y | Energy Fuels 2013, 27, 5054−5068

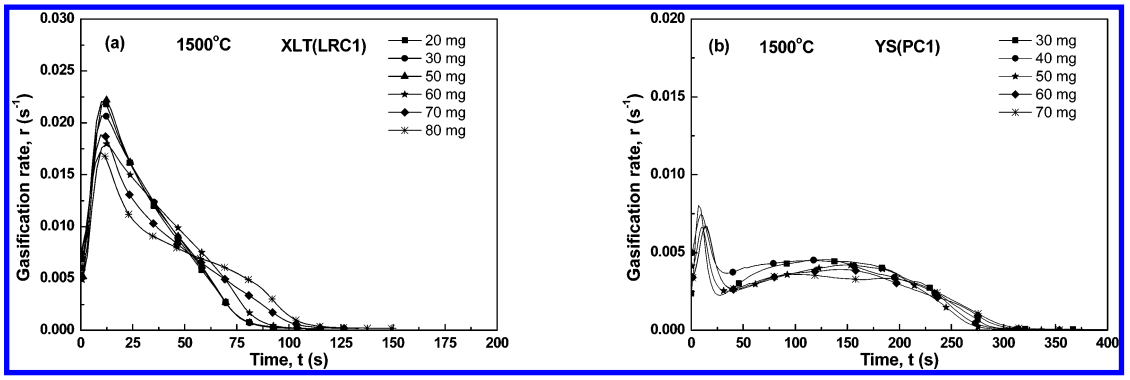

Figure 4. Comparison of the CO_2-gasification rate profiles of (a) XLT(LRC1) and (b) YS(PC1) with the different particle sizes (measured by weight) at 1500 °C under atmospheric pressure.

influence of particle size (measured by weight) on gasification rate was tested for samples XLT(LRC1) and YS(PC1) in CO_2 at 1500 °C under atmospheric pressure. Figure 4 compares the results from samples with different sizes (20−80 mg in weight, which corresponds to the particle sizes 0.7−3.5 mm). It can be seen that the effect of particle size on the gasification rate is negligible when the particle weight is less than 50 mg for sample XLT(LRC1) and is in the whole test weight range for sample YS(PC1). The particle weight of 50 mg, therefore, was selected.

Here it should be mentioned that the sample particle may burst into small pieces after being dropped into the reaction zone. Figure 5 shows the change of the particle size for some test

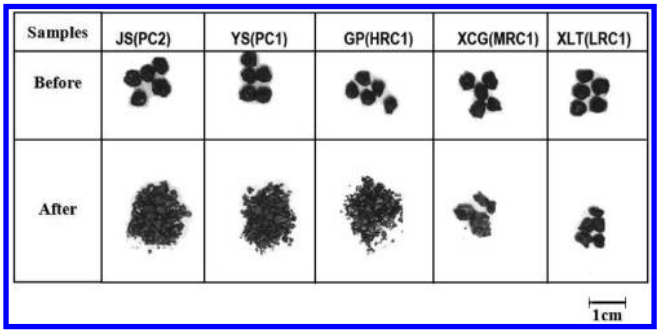

Figure 5. Photographs of the sample particles before and after being fed into the reaction zone, in which the sample was devolatilized in Ar under atmospheric pressure at 1400 °C for 5 min.

samples before and after being fed into the reaction zone of the drop-in-fixed-bed reactor, in which the sample is devolatilized in Ar under atmospheric pressure at 1400 °C for 5 min. Samples XLT(LRC1) and XCG(MRC1) are lower rank coal, sample GP(HRC1) is higher rank coal, and samples YS(PC1) and JS(PC2) are petcokes. It seems that the samples with the higher density and the lower porosity are likely to burst into small pieces. This should be a reason why the reactivity of petcoke is not sensitive to the feeding size.

3.3. Comparison of Gasification Rate Profiles of Various Coals and Petcokes. The profiles shown in Figure 6 compare the CO_2- and steam-gasification reactivities of 13 solid carbonaceous materials, including 9 coal samples (5 low-rank coals: XLT, SL, WS, TL, and YM; 1 mid-rank coal: XCG; 3 high-rank coals: GP, YQ, and QS), 2 petcoke samples (YS and JS), and 2 graphite samples (GR1 and GR2), in the temperature range 1200−1600 °C under atmospheric pressure.

In the case of CO_2-gasification (left-hand side of Figure 6), similar to that for sample XLT(LRC1), the rate profiles of all low-rank coal samples tested appear with only one tailing peak in the whole temperature range. The transition point between the region involving reactions for both volatiles and char and the region of char reaction is not distinguishable. The rate increases with time rapidly to a maximum value and then undergoes an exponential decay approaching zero as the carbon totally converted. At the low temperature (1200 °C), the rate profiles of different low-rank coals are distinguishable. As the temperature increases, the peak intensity of low-rank coal increases and the peaking time decreases. At the high temperature, the rate difference for different low-rank coals is diminished.

Unlike the low-rank coals, the rate profiles of mid- and high-rank coals are characterized with two distinguishable regions: a sharp peak followed by a broad peak (with relatively low intensity) in the temperature range 1200−1400 °C. And the rate difference among coals is distinguishable. The two-peak phenomenon is diminished as the temperature increases further. The rate difference among high-rank coals, however, is still distinguishable.

In the temperature range 1200−1600 °C, the two-peak phenomenon clearly exists for petcoke samples while no sharp peak at an early stage is observed in the rate profiles for graphite samples. This agrees with the fact that the petcoke samples are green coke, containing a certain amount of volatiles, and that the graphite samples contain little volatiles.

In the case of steam-gasification (right-hand side of Figure 6), the two-peak phenomenon is not significant in most of the cases. The rate profiles of most coals in different ranks appear with only one tailing peak in the temperature range 1200−1600 °C. However, the two-peak phenomenon clearly appears for petcokes when the temperature is less than 1500 °C and disappears at 1600 °C.

Similar to the CO_2-gasification, the rate difference among samples in the steam-gasification decreases as the temperature increases. Based on the rate profiles at 1600 °C, the samples can be separated into two groups: (1) coals; (2) petcokes and graphite. The rate difference is still visible between coal and petcoke at 1600 °C.

In general, at the lower temperature the rate difference among the different samples is apparent regardless of the gasifying reagent used. The difference decreases as the temperature increases. The higher temperature is, the less the difference is. This can be seen more clearly from the view shown in Figure 7, in which the required reaction time for a sample approaching 100% carbon conversion ratio is presented as a function of gasification temperature. Furthermore, the temperature has

dx.doi.org/10.1021/ef400373y | *Energy Fuels* 2013, 27, 5054−5068

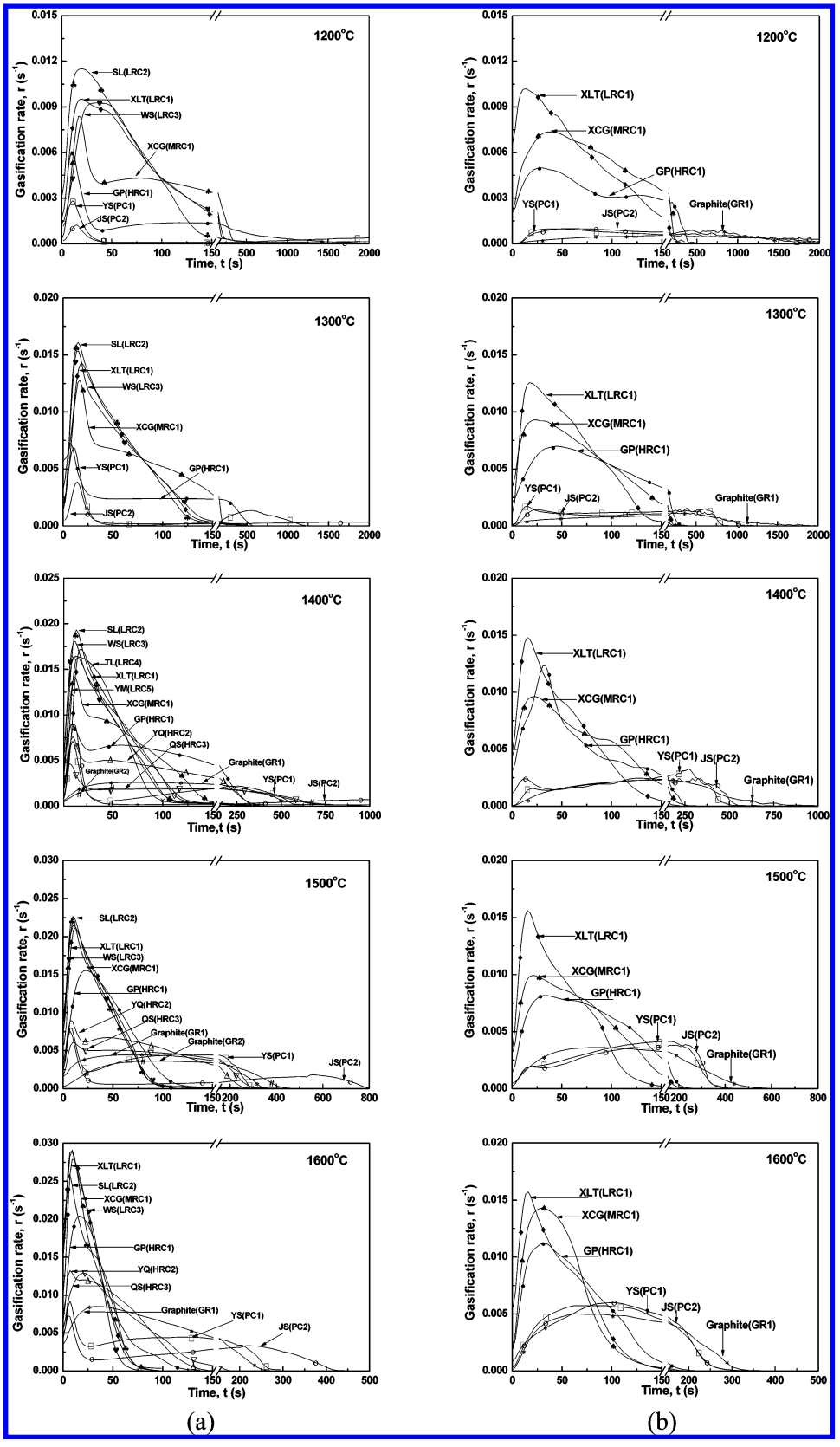

Figure 6. Dynamic gasification rate profiles of coals, petcokes, and graphites in the temperature range 1200−1600 °C under atmospheric pressure: (a) in CO_2 (100% CO_2) and (b) in steam (36% steam in Ar).

more impact on the gasification of petcokes and graphite although the gasification reactivity of petcokes and graphite is far from that of coals.

In the foregoing discussion, no comparison is made for the difference between the CO_2-gasification and the steam-gasification due to the data used in the discussion being obtained

dx.doi.org/10.1021/ef400373y | *Energy Fuels* 2013, 27, 5054−5068

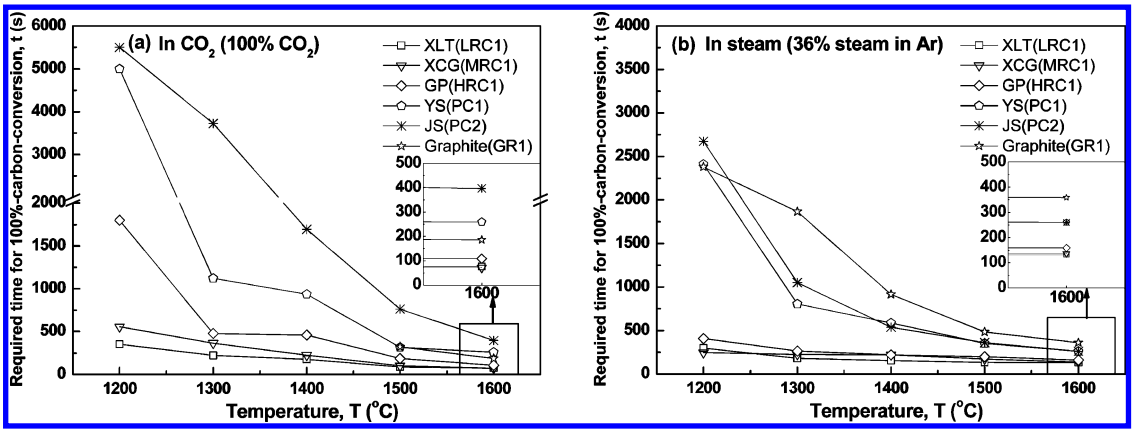

Figure 7. Required reaction time for approaching 100%-carbon-conversion at different temperatures: (a) in CO_2 (100% CO_2) and (b) in steam (36% steam in Ar).

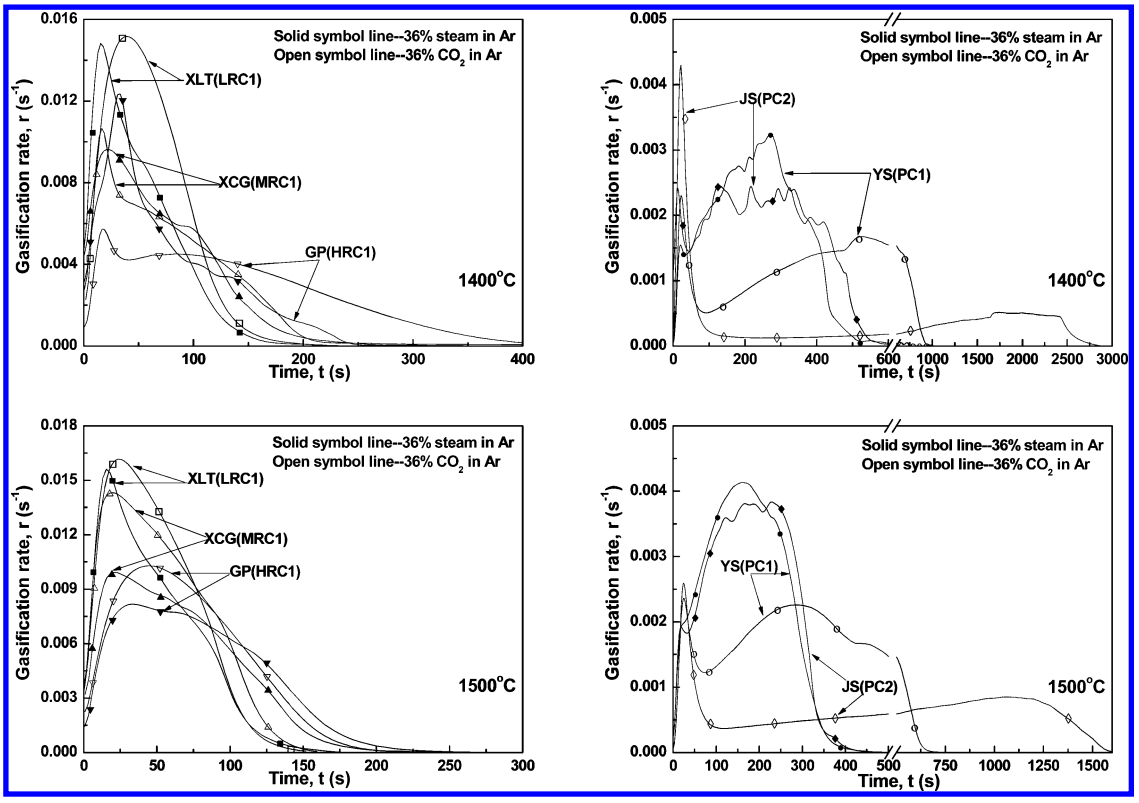

Figure 8. Dynamic CO_2- and steam-gasification rate profiles of coals and petcokes at 1400 and 1500 °C under atmospheric pressure (volumetric concentration of gasifying agent: 36% in Ar).

in pure CO_2 for the CO_2-gasification and 36% steam in Ar for the steam-gasification. Figure 8 compares the difference between the CO_2-gasification and the steam-gasification under the same volumetric concentration (36% in Ar) at 1400 and 1500 °C. It shows that at 1400 °C the steam-gasification rate for coals is slightly higher than the CO_2-gasification rate while at 1500 °C the CO_2-gasification rate for samples XCG(MRC1) and GP(HRC1) becomes slightly higher than the steam-gasification rate. From the data shown in Figure 6, a similar phenomenon, the CO_2-gasification rate is higher than the steam-gasification rate, can be observed for some coal samples at the higher temperature. However, the steam-gasification rate is higher than the CO_2-gasification rate at the lower temperature although the concentration of steam is lower than that of CO_2. This agreed with the results reported in the literature.[26,27] For petcokes, the steam-gasification rate is always much higher than the CO_2-gasification rate under the experimental condition.

Furthermore, corresponding to the carbon conversion ratio, Figure 9 compares the gasification rates of coals and petcokes with different gasifying agents (CO_2 and steam). At 1400 °C, for XLT coal the steam-gasification rate is slightly higher than the CO_2-gasification rate when the carbon conversion ratio is less than 20% while the order switches and the difference becomes significant afterward. For XCG coal, the steam-gasification rate is slightly lower than the CO_2-gasification rate when the carbon conversion is near 20% while the order switches afterward. For GP coal and petcokes the steam-gasification rate is higher than the CO_2-gasification rate in the whole carbon conversion range basically. At 1500 °C, for three coals the CO_2-gasification rate is always higher than the steam-gasification rate in the whole

dx.doi.org/10.1021/ef400373y | Energy Fuels 2013, 27, 5054−5068

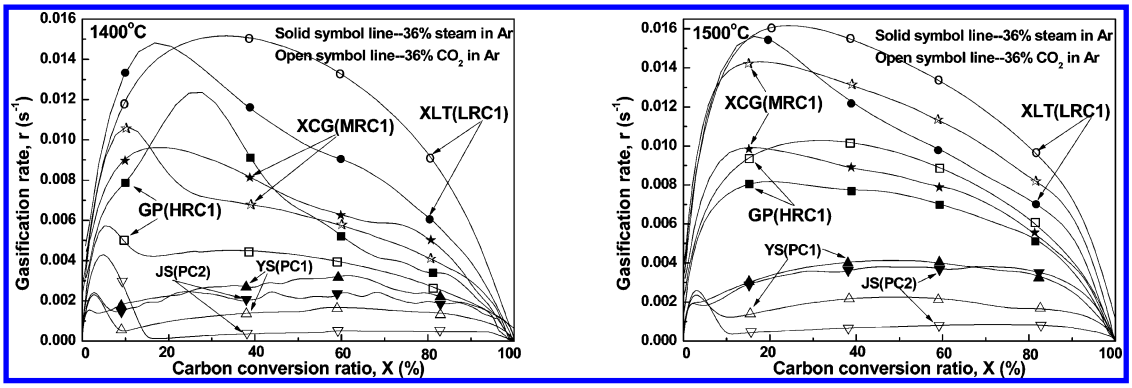

Figure 9. Comparison of the CO_2- and steam-gasification rates of coals and petcokes with respect to carbon conversion ratio at 1400 and 1500 °C under atmospheric pressure (volumetric concentration of gasifying agent: 36% in Ar).

Table 2. Gibbs Free Energies at Different Temperatures for Reactions R-1 and R-2

	Gibbs free energy (ΔG_m/kJ·mol^{-1})		
temp/°C	ΔG_{m1} (R-1: C + CO_2 → 2CO)	ΔG_{m2} (R-2: C + H_2O → CO + H_2)	$\Delta G_{m1} - \Delta G_{m2}$
727	-4.4	-7.6	3.2
827	-21.9	-21.9	0
927	-39.3	-36.3	-3
1027	-56.5	-50.6	-5.9
1127	-73.7	-64.9	-8.8
1227	-90.9	-79.2	-11.7
1327	-107.8	-93.5	-14.3
1427	-124.8	-107.7	-17.1
1527	-141.7	-121.9	-19.8
1627	-158.5	-136.1	-22.4

carbon conversion range. For petcokes the steam-gasification rate is still higher than the CO_2-gasification rate.

It is true that the results of the CO_2-gasification rate exceeding the steam-gasification rate are contrary to the common understanding. However, there is some published data implying a similar result.[25] The results from Sha's research indicate that the effect of temperature on the CO_2-gasification of a coal char sample is more significant than that on the corresponding steam-gasification; that is, the slope of Arrhenius plot for the CO_2-gasification of the sample is larger than that for the corresponding steam-gasification.[28] Therefore, it is possible that the CO_2-gasification rate of coal is higher than the corresponding steam-gasification rate when the temperature is high enough. The following three points may be used for explanation.

(a) From the thermodynamics point of view. The Gibbs free energies at different temperatures for the CO_2-gasification (R-1) and the steam-gasification (R-2) were calculated by using the FactSage software and are listed in Table 2. It shows that the reaction R-1 is more favorable than the reaction R-2 as the temperature increases.

(b) From the gas diffusion point of view. The mean free paths for CO_2 and H_2O were estimated by the kinetic theory of gases[10] and are listed in Table 3. From 1000 to 1600 °C the mean free path increases from 376 to 553 nm for CO_2 and from 556 to 818 nm for H_2O. The Knudsen diffusion is more prominent for the steam-gasification, especially at higher temperatures.

Table 3. Gas Mean Free Paths (nm) Estimated Using Kinetic Theory of Gases under Atmospheric Pressure

	1000 °C	1200 °C	1400 °C	1600 °C
CO_2	376	435	494	553
H_2O	556	643	730	818

(c) From the catalytic gasification point of view. The ash compositions of the test samples were analyzed and are listed in Table 4. The contents of alkali and alkaline earth metals (AAEMs) in coals and petcoke are very much different. The coal samples contain relatively high amounts of AAEMs, especially in sample XLT(LRC1), while the petcoke contains little AAEMs. It has been reported that the AAEMs is more active for the CO_2-gasification than that for the steam-gasification.[29]

In general, the high temperature is favorable to the CO_2-gasification. The catalytic effect of AAEMs should be a key factor. With the aid of AAEMs the gasification reactivity of coal in CO_2 may be higher than that in steam at high temperature. The limited AAEMs limit the catalytic gasification of petcoke in CO_2.

3.4. Physical Structure of Raw Samples and Their Corresponding Chars. Under the experimental conditions used in this study, the rate limiting reactions are the reactions between carbon and gasifying agent. Besides the reactivity of the reactants, the diffusion difficulty of the gasifying agent in solid carbonaceous material as well as its corresponding char is another factor affecting the overall gasification reactivity. It is a common understanding that at the high temperature the reaction between carbon and gasifying agent is fast and the diffusion of gaseous reactant and products to and from solid reactant becomes control steps. The particle size of the solid reactant is one factor affecting the gas diffusion process, which is discussed in section 3.2. The physical structure of the solid reactant (such as surface morphology and pore structure) may also be related to the gas diffusion process,[15] which is discussed in this section.

dx.doi.org/10.1021/ef400373y | Energy Fuels 2013, 27, 5054−5068

Table 4. Ash Composition Analyses of Some Test Samples[a]

sample	SiO_2	Al_2O_3	Fe_2O_3	CaO	MgO	TiO_2	SO_3	K_2O	Na_2O	P_2O_5
XLT(LRC1)	33.97	10.88	11.67	27.90	2.80	0.70	9.72	0.43	0.08	0.27
XCG(MRC1)	61.08	18.10	5.25	7.48	2.12	0.97	2.04	1.76	0.46	0.12
GP(HRC1)	51.22	33.44	3.29	5.04	0.99	1.13	2.03	1.04	0.57	0.23
YS(PC1)	8.47	–	25.33	–	–	0.63	1.34	–	–	0.42

[a]–: not detected.

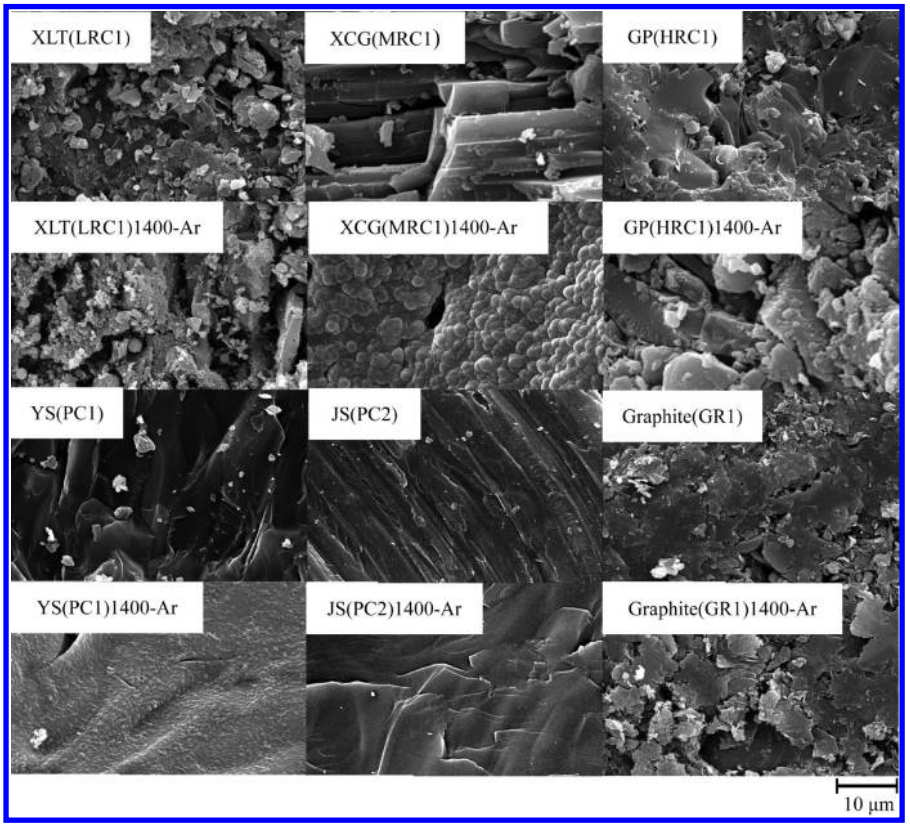

Figure 10. SEM images of raw samples and their 1400 °C Ar-heat-treated samples, which is marked as sample name1400-Ar (×2000).

Figure 10 gives scanning electron microscope (SEM) images of different raw samples and their 1400 °C Ar-heat-treated samples (prepared at 1400 °C in Ar for 5 min, marked as sample name1400-Ar) with a magnification of 2000. The SEM images reveal that the surface morphology of the coal chars and the heat-treated graphite is rougher than their parent samples' while the surface morphology of the calcined petcokes is smoother than their parent samples'. Relating the gasification reactivity shown in section 3.3 for different samples, it is important to notice that the order of the surface roughness agrees with the order of the gasification reactivity.

Actually, it can be certain that the gasification reactivity of the samples should be positively correlated with the roughness of the materials' surface since the gasification reaction is a bimolecular reaction of carbon and gasifying agent. Figure 11 compares the total pore volume and the BET surface area of some partially gasified samples in CO_2 under atmospheric pressure at 1200 °C for 1 min (marked as sample name1200-CO_2). It can also be noticed that the gasification reactivity shown in Figures 6 and 7 is positively correlated with the total pore volume and the BET surface area. These two parameters, however, cannot be correlated linearly with gasification reactivity, implying the existence of other influence factors.

Figure 12 shows the pore size distributions of foregoing partially gasified samples. It represents the detailed relationship of the pore volume and the BET surface area with the pore size. It shows that the pore volume and the BET surface area for the XLT(LRC1)1200-CO_2 sample are mainly contributed by the 3−4 nm size pores while the pore volume and the BET surface area for XCG(MRC1)1200-CO_2 and GP(HRC1)1200-CO_2 samples are mainly contributed by the pores with the size smaller than 3 nm. There is nearly no pore with the pore size larger than 2 nm in YS(PC1)1200-CO_2 and JS(PC2)1200-CO_2 samples. The high pore volume and surface area as well as larger pore size are favorable to the gas-solid reaction.

3.5. Kinetic Analysis. The overall gasification rate of solid carbonaceous materials is controlled not only by the carbon reaction but also by the contact difficulty of carbon and gasifying agents. The increase in the gasification temperature, the reaction surface, the gas diffusion rate, and the rate of mass transfer to and from the exterior of the coal particle can accelerate the carbon conversion rate. The rate-limiting mechanism varies with the gasifier or reactor used. There are many kinetic models proposed to satisfy the different situations. The shrinking core model (SCM) and the volume reaction model (VRM) were adopted for kinetic modelling in this study.

The assumption with the SCM is that the gasifying agent reacts with carbon on the external surface of a spherical particle char and the reaction surface moves toward the center of the particle

dx.doi.org/10.1021/ef400373y | *Energy Fuels* 2013, 27, 5054−5068

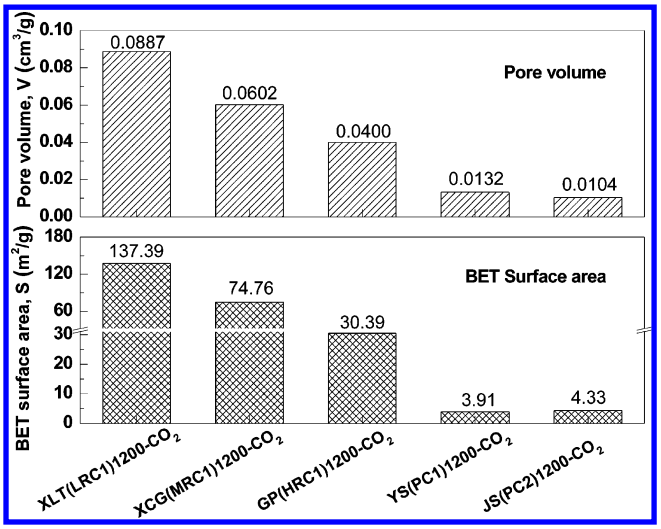

Figure 11. Surface area and pore volume of partially gasified samples.

gradually and leaves an ash layer behind.[30] As the carbon conversion proceeds, the unreacted core shrinks and diminishes when the reaction is finished. The differential equation for the SCM is expressed as follows:

$$\frac{dX}{dt} = k_s(1 - X)^{2/3} \tag{5}$$

where k_s is the overall gasification rate constant and X is the carbon conversion ratio. Its integrated form is as follows:

$$k_s t = 1 - (1 - X)^{1/3} \tag{6}$$

The assumption with the VRM is that as the gasification proceeds, the volume of the particle does not change while the density of the particle decreases uniformly. The differential equation for VRM is expressed as follows:

$$\frac{dX}{dt} = k_v(1 - X) \tag{7}$$

where k_v is the overall gasification rate constant and X is the carbon conversion ratio. Its integrated form is as follows:

$$k_v t = \ln(1 - X)^{-1} \tag{8}$$

The modelling was carried out by fitting eqs 6 and 8 with the experimental data (up to carbon conversion ratio of 95%). The plots of the SCM fitting $(1 - (1 - X)^{1/3}$versus time) are shown in Figure 13a for the CO_2-gasification and Figure 14a for the steam-gasification. The plots of the VRM fitting $(\ln(1 - X)^{-1}$ versus time) are shown in Figure 13b for the CO_2-gasification and Figure 14b for the steam-gasification. For the SCM fitting, the associated R^2 is in the range 0.9506−0.9992 for the CO_2-gasification and 0.9452−0.9998 for the steam-gasification. For the VRM fitting, the associated R^2 is in the range 0.8969−0.9984 for the CO_2-gasification and 0.8905−0.9904 for the steam-gasification.

Generally, the high R^2 values are associated with the coal samples while the low R^2 values are associated with the petcoke samples. The fitting results by the SCM seem a little better than that by the VRM. Either the SCM or the VRM is suitable for most samples and conditions but not suitable for the petcokes. The fitting results for the low-temperature data are better than that for the high-temperature data, especially for graphite and some high-rank coals. The fitting results for the CO_2-gasification data are better than that for the steam-gasification data. An apparent problem is associated with the low-reactivity samples, such as petcoke. The carbon conversion ratios predicted by either model are too high for the early stage and too low for the late stage. The gas diffusion problem, in particular, should be more significant for these samples. But there is no consideration related to the gas diffusion in the char pores in both models.

The SCM is believed as a suitable model for high-temperature gasification of solid carbonaceous materials,[16] in which the chemical reaction is very high and the rate of mass transfer to and from the exterior of the char particle is considered as the rate-limiting step. The VRM is a first-order rate model. It simplifies the heterogeneous gas−solid reaction to a homogeneous reaction throughout the solid carbonaceous particle.[31,32] The SCM assumes a strong mass transfer limited mechanism to and from the char particle while the VRM assumes a chemical reaction rate limited mechanism. A diffusion term associated with the carbon structure may be needed for better modelling the gasification behaviors of the petcoke-like materials.

The overall gasification rate constants were obtained from the slopes of the straight lines in Figures 13 and 14 and listed in Tables 5 and 6, which is a quantitative expression for the discussion given in section 3.3. Although the values of the rate constants obtained from the different models are different, the trend is consistent. As the temperature increases from 1200 to 1600 °C, for the CO_2-gasification the value of the rate constant increased about 2−4 times for low-rank coals, 5 times for mid-rank coal, 10 times for high-rank coals, and 25 times for petcoke while for the steam-gasification the value of the rate constant

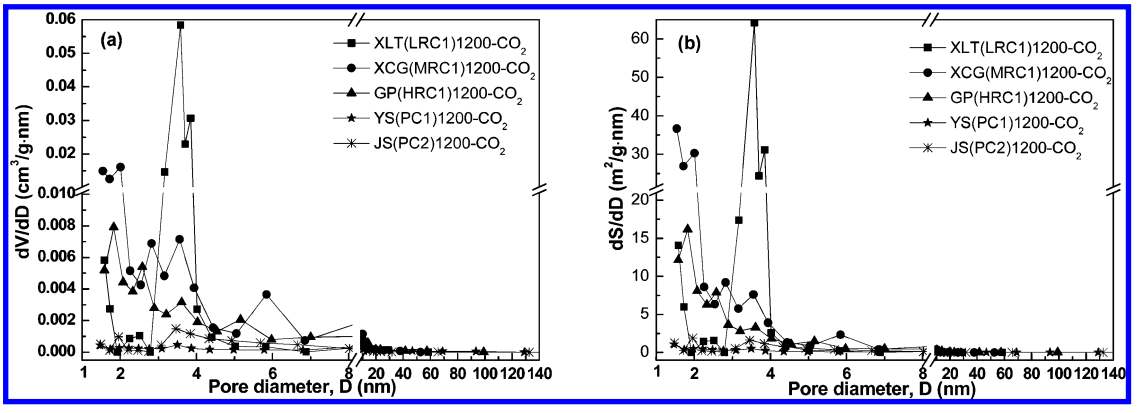

Figure 12. Pore size distributions of partially gasified samples.

dx.doi.org/10.1021/ef400373y | Energy Fuels 2013, 27, 5054−5068

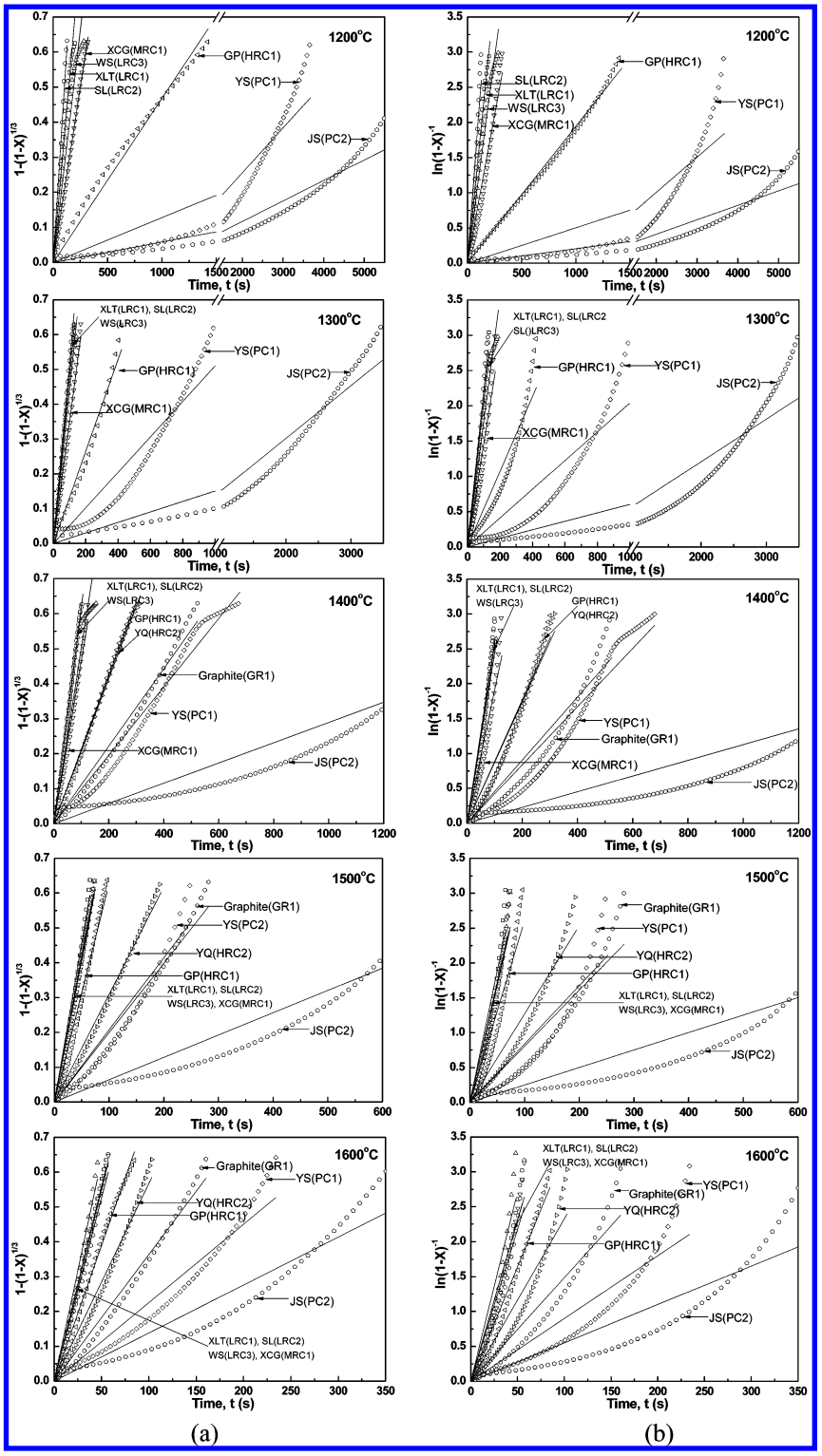

Figure 13. Plots of kinetic modelling according to (a) the SCM and (b) the VRM for the CO_2-gasification (the symbol profiles are experimental data, and the straight lines are fitting results).

increased about 1.5 times for low-rank coal, 2 times for mid-rank coal, 2.5 times for high-rank coal, and 9 times for petcokes.

At 1200 °C, the value of the rate constant of XLT(LRC1) is 65 times higher for the CO_2-gasification and 10 times higher for the steam-gasification than that of petcoke sample JS(PC2) while, at 1600 °C, the value of the rate constant of XLT(LRC1) is only 8 times higher for the CO_2-gasification and 2.5 times higher for the steam-gasification than that of petcoke sample JS(PC2). The reactivity difference among samples decreases as the temperature increases. In the temperature range 1400−1600 °C, for coals the value of the rate constant associated with the CO_2-gasification is higher than that associated with the steam-gasification while for petcoke sample JS(PC2) the value of the rate constant associated with the CO_2-gasification is lower than that associated with the steam-gasification.

dx.doi.org/10.1021/ef400373y | *Energy Fuels* 2013, 27, 5054−5068

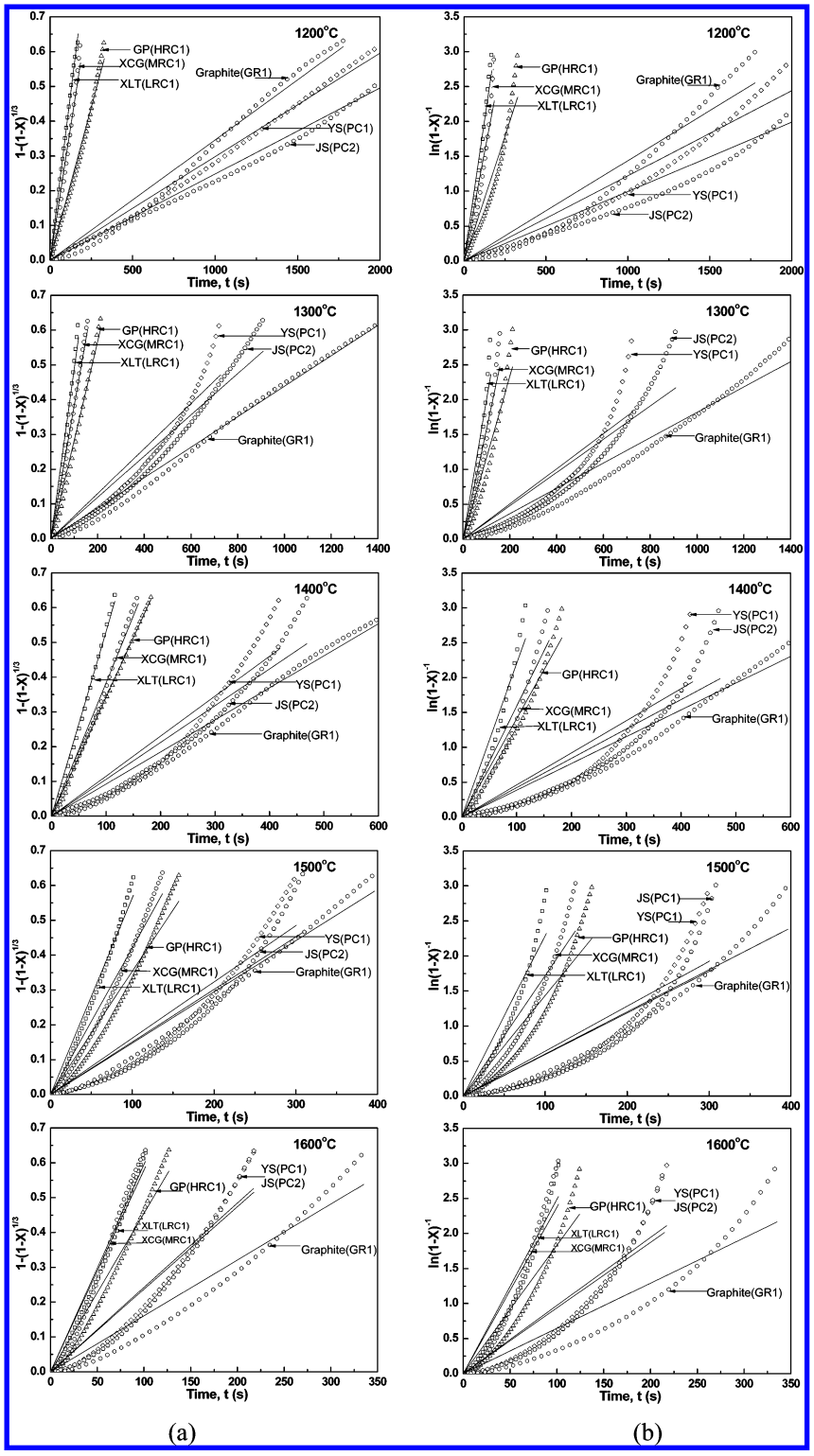

Figure 14. Plots of kinetic modelling according to (a) the SCM and (b) the VRM for the steam-gasification (the symbol profiles are experimental data, and the straight lines are fitting results).

Furthermore, through the Arrhenius equation, the rate constant, k (k_s and k_v), can be related to the apparent activation energy, E_a:

$$k = A \exp\left(-\frac{E_a}{RT}\right) \tag{9}$$

where A, R, and T are the pre-exponential factor, gas constant, and gasification temperature, respectively.

The Arrhenius plots corresponding to the rate constants shown in Tables 5 and 6 are given in Figure 15. For better fitting, the data has been split into two parts for coal samples: 1000−1200 °C and 1200−1600 °C, indicating the alteration of the gasification mechanism around 1200 °C.

The calculated apparent activation energies are listed in Table 7. The corresponding R^2 values are in the ranges 0.8657−0.9984 associated with the SCM fitting and 0.7824−0.9951

dx.doi.org/10.1021/ef400373y | Energy Fuels 2013, 27, 5054−5068

Table 5. Rate Constants, k_s or k_v (10^{-3}·s^{-1}), from the Kinetic Modelling (CO_2-Gasification)

temp/°C	model	XLT (LRC1)	SL (LRC2)	WS (LRC3)	XCG (MRC1)	GP (HRC1)	YQ (HRC2)	YS (PC1)	JS (PC2)	graphite (GR1)
1200	SCM	3.49	4.81	2.64	1.99	0.69		0.13	0.058	
	VRM	15.07	20.21	11.62	8.36	2.54		0.51	0.21	
1300	SCM	4.83	5.14	4.42	3.50	1.32		0.51	0.15	
	VRM	20.30	21.76	17.56	14.41	5.32		2.04	0.61	
1400	SCM	6.12	6.17	5.40	4.64	2.11	2.07	0.98	0.29	1.11
	VRM	25.43	25.85	24.28	19.03	8.83	8.68	4.18	1.13	4.52
1500	SCM	9.13	8.35	8.19	8.15	6.27	3.09	2.07	0.65	1.99
	VRM	37.61	34.32	33.89	33.59	26.06	12.68	8.38	2.51	8.04
1600	SCM	11.12	10.48	12.66	10.99	7.76	5.67	3.75	1.38	3.63
	VRM	46.24	43.42	54.11	46.01	32.76	23.24	12.99	5.50	14.80

Table 6. Rate Constants, k_s or k_v (10^{-3}·s^{-1}), from the Kinetic Modelling (Steam-Gasification)

temp/°C	model	XLT(LRC1)	XCG(MRC1)	GP(HRC1)	YS(PC1)	JS(PC2)	graphite(GR1)
1200	SCM	3.84	3.07	1.76	0.30	0.25	0.34
	VRM	16.11	12.45	7.15	1.22	0.99	1.44
1300	SCM	4.88	3.82	2.83	0.65	0.59	0.44
	VRM	19.93	15.71	11.64	2.52	2.39	1.82
1400	SCM	5.31	3.83	3.42	1.15	1.06	0.93
	VRM	22.01	15.87	14.08	4.60	4.21	3.84
1500	SCM	5.64	4.20	3.53	1.62	1.51	1.47
	VRM	22.91	17.19	14.34	6.41	5.93	6.01
1600	SCM	5.79	5.95	4.55	2.42	2.37	1.61
	VRM	23.73	24.86	18.30	9.72	9.36	6.45

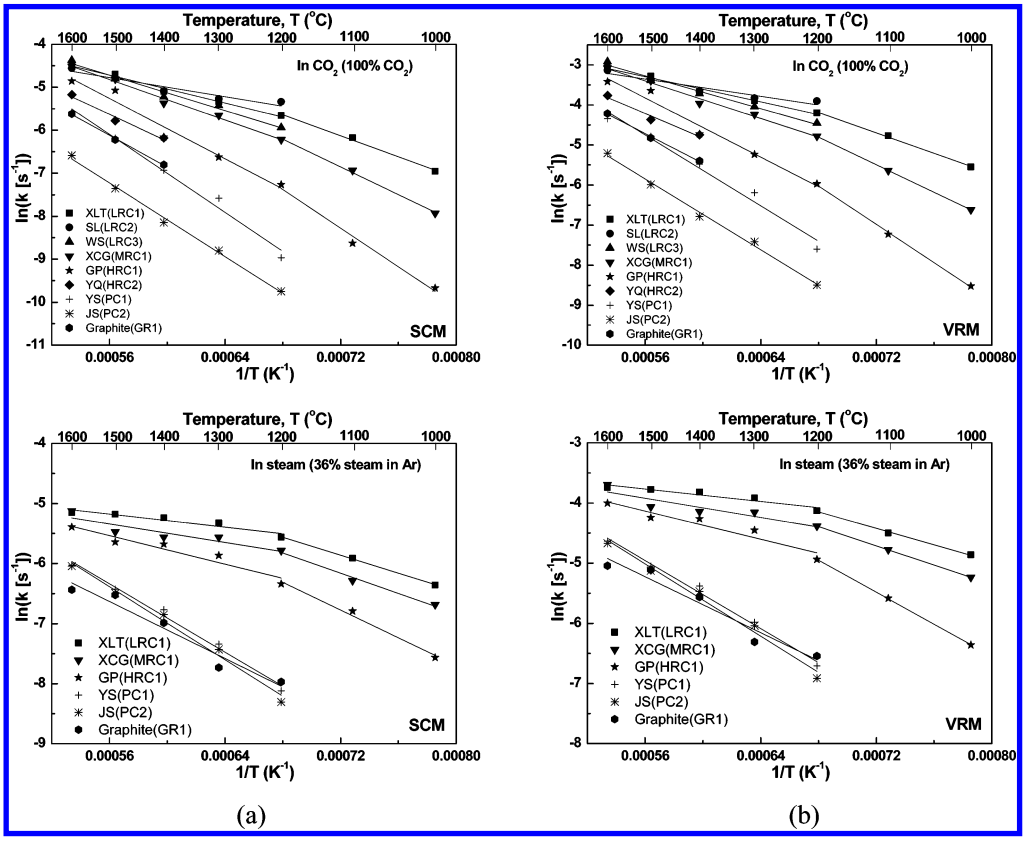

Figure 15. Arrhenius plots associated with (a) the SCM modelling and (b) the VRM modelling.

associated with the VRM fitting. The apparent activation energies from the SCM fitting are in accordance with that from the VRM fitting. The apparent activation energy corresponding to the low-temperature range is generally higher than that corresponding to the high-temperature range. The apparent activation energy corresponding to the CO_2-gasification is generally higher than that corresponding to the steam-gasification.

dx.doi.org/10.1021/ef400373y | Energy Fuels 2013, 27, 5054−5068

Table 7. Calculated Apparent Activation Energy (E_a/kJ·mol^{-1})

gasifying agent	temp/°C	XLT (LRC1)	SL (LRC2)	WS (LRC3)	XCG (MRC1)	GP (HRC1)	YQ (HRC2)	YS (PC1)	JS (PC2)	graphite (GR1)
Shrinking Core Model (SCM)										
CO_2	1000−1200	101.5			133.8	186.5				
	1200−1600	67.6	46.1	85.8	97.8	146.1	130.6	188.6	178.0	154.1
steam	1000−1200	62.1			70.0	95.8				
	1200−1600	22.7			32.0	49.3		118.2	126.2	98.5
Volume Reaction Model (VRM)										
CO_2	1000−1200	105.8			143.0	198.7				
	1200−1600	65.4	44.8	85.2	97.6	153.8	127.6	184.0	183.7	154.3
steam	1000−1200	57.0			66.3	110.6				
	1200−1600	21.5			33.2	48.7		117.5	124.8	96.7

In the temperature range 1200−1600 °C, using the SCM fitting results as an example, the apparent activation energy for the low-rank coals tested is 46.1−85.8 kJ·mol^{-1} for the CO_2-gasification and 22.7 kJ·mol^{-1} for the steam-gasification; the apparent activation energy for the mid-rank coal tested is 97.8 kJ·mol^{-1} for the CO_2-gasification and 32.0 kJ·mol^{-1} for the steam-gasification; the apparent activation energy for the high-rank coals tested is 130.6−146.1 kJ·mol^{-1} for the CO_2-gasification and 49.3 kJ·mol^{-1} for the steam-gasification; the apparent activation energy for the petcokes tested is 178.0−188.6 kJ·mol^{-1} for the CO_2-gasification and 118.2−126.2 kJ·mol^{-1} for the steam-gasification; the apparent activation energy for the graphite tested is 154.1 kJ·mol^{-1} for the CO_2-gasification and 98.5 kJ·mol^{-1} for the steam-gasification.

4. CONCLUSIONS

The comparison study was made for the CO_2- and steam-gasification reactivities of 13 carbonaceous materials in the temperature range 1000−1600 °C using a drop-in-fixed-bed reactor under atmospheric pressure. The dynamic gasification rate profile was used to characterize the gasification reactivity. The following conclusions were obtained:

(1) Like a slow-motion picture, the dynamic gasification rate profiles can clearly reveal the reactivity difference of materials and the influence of conditions, although the experimental condition is not quite close to the industrial entrained-flow gasifier. The raw materials can be used, and the problem related to prepreparation of char can be eliminated.

(2) The reactivity difference among samples decreases as the temperature increases. Up to 1600 °C, however, the gasification temperature is still a critical factor for petcokes and some high-rank coals gasifying in CO_2 or in steam, although the gasification reactivity is not distinguishable for most coals at this temperature. The kinetic analysis reveals that the temperature dependence of reactivity varies with the type of material. As the temperature increases from 1200 to 1600 °C, in the case of CO_2-gasification the rate constant increases about 2−4 times for low-rank coals, 5 times for mid-rank coal, 10 times for high-rank coals, and 25 times for petcoke while in the case of steam-gasification the rate constant increases about 1.5 times for low-rank coal, 2 times for mid-rank coal, 2.5 times for high-rank coal, and 9 times for petcokes. At 1200 °C, the rate constant of the CO_2-gasification (the steam-gasification) for XLT(LRC1) coal is 65 (10) times higher than that for JS(PC2) petcoke while at 1600 °C, the rate constant of the CO_2-gasification (the steam-gasification) for XLT(LRC1) coal is only 8 (2.5) times higher than that for JS(PC2) petcoke.

(3) In the temperature range 1400−1600 °C, for coals the rate constant associated with the CO_2-gasification is higher than that associated with the steam-gasification while for petcoke sample JS(PC2) the rate constant associated with the CO_2-gasification is lower than that associated with the steam-gasification. From the views of the reaction thermodynamics, the gas diffusion difficulty, and the catalytic effect, the high temperature is favorable to the CO_2-gasification. The effect of AAEMs (alkali and alkaline earth metals) should be a key factor. The content of AAEMs is apparent in coals and it is limited in petcokes. The limited AAEMs limit the catalytic gasification of petcokes in CO_2.

(4) The Arrhenius plot reveals that the gasification mechanism has may be altered around 1200 °C for most coal samples. The apparent activation energy corresponding to the low-temperature range is generally higher than that corresponding to the high-temperature range. The apparent activation energy corresponding to the CO_2-gasification is generally higher than that corresponding to the steam-gasification. In the temperature range 1200−1600 °C, the apparent activation energy for the low-rank coals tested is 46.1−85.8 kJ·mol^{-1} for the CO_2-gasification and 22.7 kJ·mol^{-1} for the steam-gasification; the apparent activation energy for the mid-rank coal tested is 97.8 kJ·mol^{-1} for the CO_2-gasification and 32.0 kJ·mol^{-1} for the steam-gasification; the apparent activation energy for the high-rank coals tested is 130.6−146.1 kJ·mol^{-1} for the CO_2-gasification and 49.3 kJ·mol^{-1} for the steam-gasification; the apparent activation energy for the petcokes tested is 178−188.6 kJ·mol^{-1} for the CO_2-gasification and 118.2−126.2 kJ·mol^{-1} for the steam-gasification; the apparent activation energy for the graphite tested is 154.1 kJ·mol^{-1} for the CO_2-gasification and 98.5 kJ·mol^{-1} for the steam-gasification.

(5) The gasification reactivity is related to the physical structure of the samples, including the surface morphology, the surface area, the pore volume, and the pore distribution. The petcokes with the most compact physical structure have the least gasification reactivity. The gasification reactivity is positively correlated with the total pore volume and the BET surface area. But no linear relationship can be found, indicating the complexity of the influence factors.

(6) Many factors can influence the gasification behavior of solid carbonaceous materials. The overall gasification rate can be limited by the surface chemical reaction, the rate of diffusion in the char pores, and the rate of mass transfer to and from the exterior of the char particles. The surface chemical reaction can be affected by the surface adsorption and the surface diffusion. Either the shrinking core model (SCM) or the volume reaction model (VRM) is suitable for most of the samples and conditions but not suitable for the petcokes. The fitting results for the low-temperature data are better than those for the high-temperature

dx.doi.org/10.1021/ef400373y | Energy Fuels 2013, 27, 5054−5068

data, especially for graphite and some high-rank coals. The fitting results for the CO_2-gasification data are better than those for the steam-gasification data. The slow overall gasification rate and the poor kinetic fitting results may indicate the importance of the reactive gas diffusion in the char pores for materials such as petcoke. A diffusion term associated with the carbon structure may be needed for modelling the gasification behaviors of the petcoke-like materials.

AUTHOR INFORMATION

Corresponding Author

*Tel./fax: +86 351 4048571. E-mail: jyang@sxicc.ac.cn.

Notes

The authors declare no competing financial interest.

ACKNOWLEDGMENTS

The authors gratefully acknowledge the financial support from the National Basic Research Program of China (2010CB227003) and the Natural Science Foundation of China (21176244). Bijiang Zhang, Baoqing Li, Yunmei Li, Hongxian Niu, and Wenzhong Shen of Institute of Coal Chemistry, Chinese Academy of Sciences, are acknowledged for their valuable suggestions and help with experiments.

REFERENCES

(1) Li, F.; Fan, L. *Energy Environ. Sci.* **2008**, *1*, 248−267.
(2) Irfan, M. F.; Usman, M. R.; Kusakabe, K. *Energy* **2011**, *36*, 12−40.
(3) Mondal, P.; Dang, G.; Garg, M. *Fuel Process. Technol.* **2011**, *92*, 1395−1410.
(4) Minchener, A. J. *Fuel* **2005**, *84*, 2222−2235.
(5) Roberts, D.; Hodge, E.; Harris, D.; Stubington, J. *Energy Fuels* **2010**, *24*, 5300−5308.
(6) Cetin, E.; Gupta, R.; Moghtaderi, B. *Fuel* **2005**, *84*, 1328−1334.
(7) Miura, K.; Hashimoto, K.; Silveston, P. *Fuel* **1989**, *68*, 1461−1475.
(8) Huttinger, K.; Nattermann, C. *Fuel* **1994**, *73*, 1682−1684.
(9) Li, C. *Fuel* **2007**, *86*, 1664−1683.
(10) Bell, D. A.; Towler, B. F.; Fan, M. *Coal gasification and its applications*; Elsevier: Oxford, U.K., 2011; pp 35−56.
(11) Liu, H.; Kaneko, M.; Luo, C.; Kato, S.; Kojima, T. *Fuel* **2004**, *83*, 1055−1061.
(12) Gale, T. K.; Bartholomew, C. H.; Fletcher, T. H. *Energy Fuels* **1996**, *10*, 766−775.
(13) Peng, F.; Lee, I.; Yang, R. *Fuel Process. Technol.* **1995**, *41*, 233−251.
(14) Molina, A.; Mondragon, F. *Fuel* **1998**, *77*, 1831−1839.
(15) Hodge, E.; Roberts, D.; Harris, D.; Stubington, J. *Energy Fuels* **2010**, *24*, 100−107.
(16) Kim, Y. T.; Seo, D.; Hwang, J. *Energy Fuels* **2011**, *25*, 5044−5054.
(17) Ahn, D.; Gibbs, B.; Ko, K.; Kim, J. *Fuel* **2001**, *80*, 1651−1658.
(18) Wu, S.; Gu, J.; Zhang, X.; Wu, Y.; Gao, J. *Energy Fuels* **2008**, *22*, 199−206.
(19) Liu, H.; Luo, C.; Kato, S.; Uemiya, S.; Kaneko, M.; Kojima, T. *Fuel Process. Technol.* **2006**, *87*, 775−781.
(20) Zhan, X.; Jia, J.; Zhou, Z.; Wang, F. *Energy Convers. Manage.* **2011**, *52*, 1810−1814.
(21) Yoon, S. J.; Choi, Y. C.; Lee, S. H.; Lee, J. G. *Korean J. Chem. Eng.* **2007**, *24*, 512−517.
(22) Takarada, T.; Tamai, Y.; Tomita, A. *Fuel* **1985**, *64*, 1438−1442.
(23) Kajitani, S.; Suzuki, N.; Ashizawa, M.; Hara, S. *Fuel* **2006**, *85*, 163−169.
(24) Miura, K.; Makino, M.; Silveston, P. *Fuel* **1990**, *69*, 580−589.
(25) Liu, H.; Zhu, H.; Kaneko, M.; Kato, S.; Kojima, T. *Energy Fuels* **2010**, *24*, 68−75.
(26) Roberts, D.; Harris, D. *Energy Fuels* **2006**, *20*, 2314−2320.
(27) Zhang, L.; Huang, J.; Fang, Y.; Wang, Y. *Energy Fuels* **2006**, *20*, 1201−1210.
(28) Sha, X.; Yang, N. *Coal Gasification and Application*; East China University of Science and Technology Press: ShangHai, 1995; pp 23−33.
(29) Ye, D.; Agnew, J.; Zhang, D. *Fuel* **1998**, *77*, 1209−1219.
(30) Heesink, A.; Prins, W.; Van Swaaij, W. *Chem. Eng. J.* **1993**, *53*, 25−37.
(31) Dutta, S.; Wen, C.; Belt, R. *Ind. Eng. Chem. Process Des. Dev.* **1977**, *6*, 20−30.
(32) Schmal, M.; Monteiro, J. L. F.; Castellan, J. L. *Ind. Eng. Chem. Process Des. Dev.* **1982**, *21*, 256−266.